

## Dimensional crossover in Bragg scattering from an optical lattice

S. Slama, C. von Cube, A. Ludewig, M. Kohler, C. Zimmermann, and Ph. W. Courteille  
*Physikalisches Institut, Eberhard-Karls-Universität Tübingen, Auf der Morgenstelle 14, D-72076 Tübingen, Germany*  
 (Received 7 June 2005; published 14 September 2005)

We study Bragg scattering at one-dimensional (1D) optical lattices. Cold atoms are confined by the optical dipole force at the antinodes of a standing wave generated inside a laser-driven high-finesse cavity. The atoms arrange themselves into a chain of pancake-shaped layers located at the antinodes of the standing wave. Laser light incident on this chain is partially Bragg reflected. We observe an angular dependence of this Bragg reflection which is different from what is known from crystalline solids. In solids, the scattering layers can be taken to be infinitely spread (three-dimensional limit). This is not generally true for an optical lattice consistent of a 1D linear chain of pointlike scattering sites. By an explicit structure factor calculation, we derive a generalized Bragg condition, which is valid in the intermediate regime. This enables us to determine the aspect ratio of the atomic lattice from the angular dependence of the Bragg scattered light.

DOI: [10.1103/PhysRevA.72.031402](https://doi.org/10.1103/PhysRevA.72.031402)

PACS number(s): 42.50.Vk, 42.55.-f, 42.60.Lh, 34.50.-s

Bragg scattering is a widely used method for observing and analyzing periodic structures. Introduced by von Laue and Bragg more than 80 years ago, it has become an inestimable tool in solid-state physics and crystallography [1]. In quantum optics, the advent of powerful laser cooling and trapping techniques has led to the realization of *optical lattices*, i.e., periodic arrangements of ultracold atoms confined to arrays of optical potentials formed by one or more standing light waves [2]. Optical Bragg scattering from three-dimensional optical lattices has been first investigated by Birkel *et al.* and Weidemüller *et al.* [3,4]. Bragg scattering from a one-dimensional (1D) optical lattice has been realized recently within our group [5]. At present, optical lattices play an important role in many experiments. The observation of Bloch oscillations [6] and the realization of Mott insulators [7] and Tonks–Girardeau gases [8] in degenerate atomic quantum gases are prominent examples. One-dimensional optical lattices have interesting effects on the collective behavior of Bose–Einstein condensates [9]. Bragg diffraction represents a powerful tool for sensitively probing the properties of such optical lattices. A method for phase-sensitive Bragg spectroscopy based on heterodyning the Bragg-reflected light with a reference light field has recently been presented by our group [5].

In this paper, we show how the Bragg condition—well known from diffraction experiments with x rays at solids—has to be modified, if the size of the crystal is limited. This is done by an explicit calculation of the structure factor. We experimentally test our model by probing the angular dependence of the Bragg condition on a 1D optical lattice. This enables us to determine the aspect ratio of the atomic lattice. We find that our optical lattice occupies an intermediate position between a linear chain of pointlike scatterers and a stack of extended homogeneous reflection layers reminiscent to a dielectric mirror.

The optical layout of our experiment is shown in Fig. 1. It consists of an optical cavity and a setup for Bragg scattering. The cavity input coupler has a curvature  $\rho_{ic}=50$  cm and a transmission  $T_{ic}=0.2\%$ , and the high reflecting mirror is plane and has a transmission  $T_{hr}=5\times 10^{-6}$ . The measured finesse of the cavity is 4000, and the beam diameter at its

center is  $w_{dip}=220$   $\mu\text{m}$ . The light of a titanium–sapphire laser operating at  $\lambda_{dip}=811$  nm is coupled and frequency locked to the cavity, thus forming a standing wave with periodicity  $(1/2)\lambda_{dip}=\pi/k_{dip}$ . The intracavity power is  $P_{cav}=5$  W. Between  $N_{tot}=10^5$  and  $10^7$   $^{85}\text{Rb}$  atoms can be loaded from a standard magneto-optical trap into the standing wave, which is red detuned with respect to the rubidium  $D_1$  line. From absorption spectroscopy of the atomic cloud, we roughly estimate that about 10 000 antinodes are filled with atoms. Typically, the temperature of the cloud is on the order of a few 100  $\mu\text{K}$ ; we noticed in earlier experiments [10,11] that the temperature of the cloud tends to adopt a fixed ratio with the depth of the dipole trap. Therefore, the spatial distribution of the atoms does not vary much with the chosen potential depth. For the trap in this setup, we measured  $k_B T \approx 0.4 U_0$ . From this, we derive the root-mean-square size of the atomic layers,  $2\sigma_z = (1/\pi)\lambda_{dip}\sqrt{k_B T/2U_0} \approx 115$  nm in the harmonic approximation of the trapping potential. The radial size is  $2\sigma_r = w_{dip}\sqrt{k_B T/U_0} \approx 140$   $\mu\text{m}$  and the mean density can be adjusted between  $n=3\times 10^9$  and  $3\times 10^{11}$   $\text{cm}^{-3}$ .

The light used to probe the Bragg resonance is generated with a near-infrared laser diode operating at  $\lambda_{brg}=780$  nm. The frequency is tuned to the Rb  $D_2$  line. The laser light is collimated to a beam waist of  $w_{brg}=800$   $\mu\text{m}$  before crossing the standing wave under an angle of  $\beta_i = \arccos(\lambda_{brg}/\lambda_{dip}) = 15.9^\circ$ . The irradiated light intensity is, with a total laser power of  $P_i=300$  nW, far below the saturation intensity.

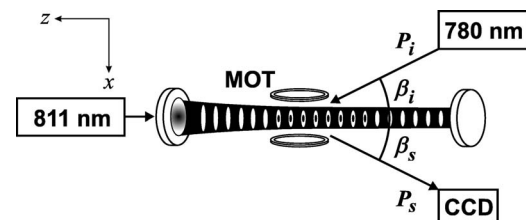


FIG. 1. The experimental setup consists of a cavity pumped at 811 nm and a diode laser at 780 nm for Bragg scattering. The Bragg-reflected light is observed on a CCD camera.

Some time after loading the atoms into the standing wave the Bragg light beam is switched on. The light reflected from the atoms,  $P_s$  (several nW), is detected with a charge coupled device (CCD) camera (Sony XC55), from which we get the intensity profile of the reflected light beam. This allows us to determine the reflection angle  $\beta_s$ .

The Bragg condition follows from energy and momentum conservation. Our standing wave dipole trap represents a 1D optical lattice with the lattice constant  $\mathbf{d} = \frac{1}{2}\lambda_{\text{dip}}\hat{\mathbf{e}}_z = d\hat{\mathbf{e}}_z$ . The Bragg condition requires that the difference between the scattered and the incident wave vectors,  $\mathbf{q} \equiv \mathbf{k}_s - \mathbf{k}_i$ , coincides with a vector of the reciprocal grating  $\mathbf{R}_j = j\mathbf{G}$ , where  $\mathbf{G} \equiv 2k_{\text{dip}}\hat{\mathbf{e}}_z$ . This implies

$$\frac{1}{2}\lambda_{\text{dip}} \cos \beta_i + \frac{1}{2}\lambda_{\text{dip}} \cos \beta_s = \lambda_{\text{brg}},$$

$$\beta_i = -\beta_s. \quad (1)$$

The first equation is the condition for constructive interference of light reflected from subsequent scattering planes. The second equation arises from the fact that the radial atomic distribution is nearly homogeneous on the length scale of a wavelength. Together, Eq. (1) yields

$$\lambda_{\text{dip}} \cos \beta_i = \lambda_{\text{brg}}. \quad (2)$$

The efficiency of Bragg scattering depends critically on the angle of incidence  $\beta_i$ . In order to probe the Bragg condition,  $\beta_i$  has to be varied over the value given by Eq. (2). Experimentally, it is easier to vary the wavelength of the lattice laser  $\lambda_{\text{dip}}$ , while the angle of incidence is kept fixed. To resonantly enhance the Bragg scattering, which otherwise would be negligibly small, we tune the laser to the transition between  $5S_{1/2}, F=3$  and  $5P_{3/2}, F'=4$  at  $\lambda_{\text{brg}}=780$  nm with a natural linewidth of  $\Gamma_{\text{brg}}/2\pi=6$  MHz. During the Bragg pulse sequence, the repumping laser of the magneto-optical trap is kept on to avoid optical pumping into the ground state  $F=2$  level.

The Bragg condition (1) implies two equations. Their claim is that for infinitely extended layers the angle of incidence and the reflection angle are equal and their cosines sum up to a fixed value. Both conditions are fulfilled, if the incident beam is shone under the Bragg angle given by Eq. (2) onto the atomic cloud. However, when the angle of incidence is misaligned from the Bragg condition, one of these equations must be violated. Which one it is depends on the form of the atomic cloud. For radially extended clouds, we expect the two angles to be equal. In contrast, for long lattices (many layers) we expect that the sum of the angles stays constant. This can be illustrated with a calculation of the structure factor  $S(\mathbf{q})$ . Its absolute square is proportional to the scattered light intensity [12],

$$\frac{dP}{d\Omega} \propto |S(\mathbf{q})|^2 = \left| \int_V n_a(\mathbf{r}) e^{i\mathbf{q}\cdot\mathbf{r}} d^3\mathbf{r} \right|^2, \quad (3)$$

where  $n_a(\mathbf{r})$  is the atomic density within the lattice. We assume for each layer a Gaussian density distribution, which is well fulfilled in the harmonic approximation

$$n_l(\mathbf{r}) = n_0 e^{(-x^2-y^2)/2\sigma_r^2} e^{-z^2/2\sigma_z^2}. \quad (4)$$

The atoms are spread over  $N_s$  layers of the lattice yielding an overall density distribution, which can be expressed as a convolution of the single site distribution with a sum of  $\delta$ -functions,

$$n_a(\mathbf{r}) = \sum_{m=1}^{N_s} \delta(\mathbf{r} - m\mathbf{d}) \star n_l(\mathbf{r}). \quad (5)$$

Inserting Eq. (5) into Eq. (3) gives

$$|S|^2 = \left| \sum_{m=1}^{N_s} e^{im\mathbf{q}\cdot\mathbf{d}} \int_V n_l(\mathbf{r}) e^{i\mathbf{q}\cdot\mathbf{r}} d^3\mathbf{r} \right|^2. \quad (6)$$

The sum in Eq. (6) can be written as an Airy function

$$|A|^2 = \left| \sum_{m=1}^{N_s} e^{imq_z d} \right|^2 = \frac{1 - \cos(N_s q_z d)}{1 - \cos(q_z d)}. \quad (7)$$

Experimentally relevant is first-order scattering  $q_z d = 2\pi$ , for which the Airy function reaches a maximum with an approximated full width at half height of  $2\delta k_z = 2\sqrt{3(5-\sqrt{5})}/N_s d \approx 2 \times 2.88/N_s d$ . For this approximation, the cosines of the Airy function are expanded up to sixth order and  $N_s \gg 1$ . The integrals in Eq. (6), one for every direction in space, are evaluated functions, for example,

$$|B(q_x)|^2 \equiv \left| \int e^{iq_x x} e^{-x^2/2\sigma_r^2} dx \right|^2 = 2\pi\sigma_r^2 e^{-q_x^2\sigma_r^2}. \quad (8)$$

On Bragg resonance  $q_x = q_y = 0$  and  $q_z = 2k_{\text{dip}}$ . The full width at half height of  $|B(q_x)|^2$  and  $|B(q_y)|^2$  is given by  $2\delta k_{x,y} = 2\sqrt{\ln 2}/\sigma_r$ . The Debye-Waller factor  $|B(q_z)|^2$  can be regarded as a constant attenuation of the structure factor within the above calculated range  $2\delta k_z$ .

The above calculated widths  $\delta k_{x,y,z}$  correspond to a certain solid angle  $\Omega$ , into which the Bragg-scattered light is emitted. The solid angle is given by  $\Omega = \pi\phi_1\phi_2$ , with the half opening angles  $\phi_1, \phi_2 \ll 1$ . The situation is simple for the  $y$  direction, which is orthogonal to the scattering plane:  $\phi_1 \approx \delta k_y/k_{\text{brg}}$ . Within the scattering plane, the widths  $\delta k_x$  and  $\delta k_z$  have to be projected onto a plane orthogonal to the emission direction, as shown in Fig. 2. The opening angle  $\phi_2$  is then determined by the maximum of the two projections:  $\phi_2 = \max\{(\delta k_x/k_{\text{brg}})\cos\beta_s, (\delta k_z/k_{\text{brg}})\sin\beta_s\}$ . The total result for the solid angle is therefore

$$\Omega = \pi \frac{\sqrt{\ln 2}}{\sigma_r k_{\text{brg}}^2} \max \left\{ \frac{\sqrt{\ln 2}}{\sigma_r} \cos \beta_s, \frac{2.88}{N_s d} \sin \beta_s \right\}. \quad (9)$$

In our case  $(\sqrt{\ln 2}/\sigma_r)\cos\beta_s \gg (2.88/N_s d)\sin\beta_s$ , i.e., the lattice behaves more like a linear chain of pointlike scatterers. We find  $\Omega = 6.6 \times 10^{-6}$  sr. We now calculate the direction of the emitted light beam. To this purpose, we assume that the structure factor is an ellipsoid with Gaussian profile

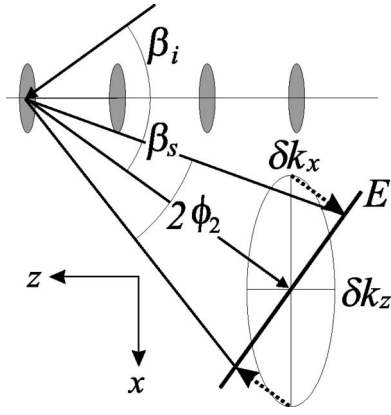


FIG. 2. Bragg reflection in real space. The gray ellipsoids symbolize the atomic layers. Within the scattering plane the opening angle  $2\phi_2$  of the Bragg beam is found by projecting the widths  $\delta k_x$  and  $\delta k_z$  onto a plane  $E$  orthogonal to the emission direction. The size of the angle is given by the larger of the two projections, here  $\delta k_x$ .

$$S = S_0 \exp \left( - \frac{(k \sin \beta_s - k \sin \beta_i)^2}{2 \delta k_x^2} - \frac{(k \cos \beta_s - 2k_{\text{dip}} + k \cos \beta_i)^2}{2 \delta k_z^2} \right), \quad (10)$$

and search for the angle  $\beta_s$ , for which the structure factor gets largest on the intersection of the ellipsoid with the Ewald sphere (see Fig. 3). Implicitly contained is the assumption that the scattering is elastic by setting  $k_i = k_s = k_{\text{brg}}$ . The part vertical to the scattering plane ( $y$  direction) is omitted, because its effect on the scattering angle is negligible. Maximization of Eq. (10),  $\partial S / \partial \beta_s = 0$ , results in

$$\delta k_z^2 - \delta k_x^2 = \frac{\delta k_z^2 \sin \beta_i}{\sin \beta_s} + \left( \cos \beta_i - \frac{2k_{\text{dip}}}{k_{\text{brg}}} \right) \frac{\delta k_x^2}{\cos \beta_s}. \quad (11)$$

Two limiting cases are interesting: For small aspect ratios,  $\delta k_z / \delta k_x \ll 1$ , we recover the Bragg condition

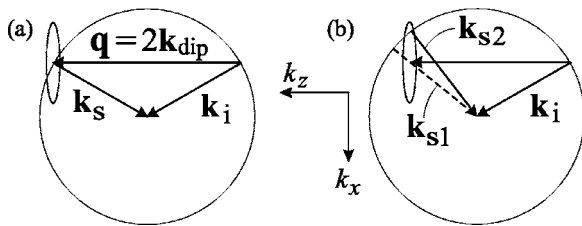


FIG. 3. Bragg reflection in reciprocal space. The pictures show cuts through the Ewald sphere and the ellipsoid structure factor. In (a), the probe laser frequency and angle fulfill the Bragg condition. In (b), the lattice constant has changed. The outgoing wave vector  $k_{s1}$  has been chosen such that  $\beta_s = -\beta_i$ , the wave vector  $k_{s2}$  such that  $\cos \beta_s + \cos \beta_i = 2\lambda_{\text{brg}} / \lambda_{\text{dip}}$ . The light will be emitted in the direction where the structure factor reaches its maximum on the intersection with the Ewald sphere.

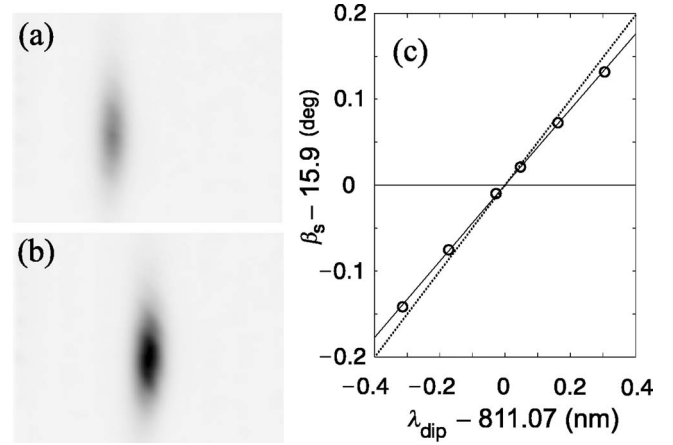


FIG. 4. (a) and (b) CCD pictures of the Bragg-reflected light for two different lattice constants. By fitting a Gaussian curve to the picture (not shown here) the center position of the beam is determined. From the displacement of the beams the relative emission angle of the light beams is calculated. (c) Output angle as a function of lattice constant. The measured values (rings) are compared to various curves: The horizontal line is expected for  $\beta_s = -\beta_i$ , the dotted line for condition (12), and finally the solid line takes account of the finite lattice size and is a fit of Eq. (14) to the data points. The fitting parameter is the aspect ratio  $\zeta$ . The experimental error of the data points lies well within the plotted circles.

$$\beta_s \approx \arccos(2k_{\text{dip}}/k_{\text{brg}} - \cos \beta_i). \quad (12)$$

For large aspect ratios,  $\delta k_z / \delta k_x \gg 1$ , we get the second of Eq. (1)

$$\beta_s \approx -\beta_i. \quad (13)$$

The impact of a finite structure factor can be seen in experiment. There are two signatures: (1) The reflection angle should deviate from the values predicted by the classical Bragg condition (1), and (2) the efficiency of the Bragg scattering should exhibit a narrow resonance upon tuning the lattice constant via  $\lambda_{\text{dip}}$ . The width of this resonance is given by the radial spread of the layers within the lattice. These signatures are observed in the following measurements.

In order to detune the Bragg condition, we vary the lattice constant via the wavelength of the lattice laser. For each lattice constant, the Bragg-diffracted light is shone onto a CCD camera [see Figs. 4(a) and 4(b)]. By fitting a Gaussian curve to a horizontal cut through the image, we get the center position of the beam. The pixel size of the camera is  $l_{\text{px}} = 7.4 \mu\text{m}$ . Together with the distance between camera and atomic cloud, we determine the relative emission angle of the Bragg beam for various lattice constants. Figure 4(c) shows that the reflection angle varies with the lattice constant, thus  $\beta_s \neq -\beta_i$ . Furthermore, the reflection angle slightly deviates from Eq. (2) (dotted line), but follows the generalized Bragg condition (11) (solid line). The findings demonstrate that our system is far from the assumption of infinitely extended layers. By introducing the aspect ratio  $\zeta = \delta k_z^2 / \delta k_x^2$ , Eq. (11) is rewritten as

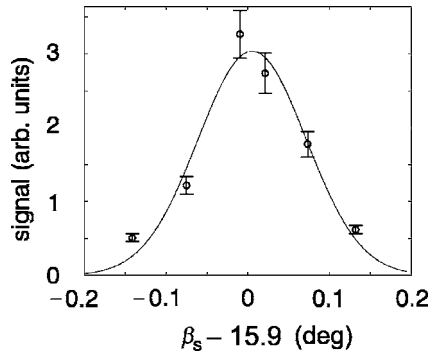


FIG. 5. Intensity of the reflected light against emission angle. The data points (circles) are fitted with a Gaussian curve. The acceptance angle of the Bragg reflection equals the width of this fit. The error of the data points is due to shot-to-shot fluctuation and lies in the 20% range.

$$\frac{1}{\zeta - 1} \left( \zeta \frac{\sin \beta_i}{\sin \beta_s} + \frac{\cos \beta_i - 2 \frac{k_{\text{dip}}}{k_{\text{brg}}}}{\cos \beta_s} \right) = 1. \quad (14)$$

By fitting the data from Fig. 4(c) with Eq. (14) (fitting parameter  $\zeta$ ), we get an aspect ratio of  $\zeta=0.01$ . This means that the ratio of the width to the length of the lattice  $2\sigma_r/N_s d=2.9\%$ . The radial size is approximately  $2\sigma_r \approx 140 \mu\text{m}$ , we therefore calculate a lattice length of  $N_s d=4.8 \text{ mm}$ . This means that about  $N_s=12\,000$  layers take part in the Bragg scattering process, which exceeds our rough guess of the lattice length by 20%. The comparatively narrow radial atomic distribution implies a self-adjustment of the Bragg condition to the lattice constant, i.e.,  $\cos \beta_s + \cos \beta_i$  is automatically kept constant. Still, small deviations from this situation [dotted line in Fig. 4(c)] are experimentally seen.

The tolerance for the acceptance angle is equal to the divergence of the outgoing beam  $2\phi_2$ . As can be seen

from the calculation of the output solid angle [Eq. (9)]  $2\phi_2=2\sqrt{\ln 2}/\sigma_r k_{\text{brg}}=0.17^\circ$ . To compare this value with the experimental data, the intensity of the reflected light extracted from Figs. 4(a) and 4(b) is plotted against the emission angle. These data are then fitted by a Gaussian curve (see Fig. 5). The full width at half maximum of this fit is  $2\delta\beta=0.16^\circ$ , which agrees very well with the theoretical value of  $2\phi_2$ .

In conclusion, we studied Bragg reflection at a 1D optical lattice. From a structure factor calculation, we deduce a generalized Bragg condition which is valid not only in the solid-state physics limit of infinitely spread scattering layers, but also for the case where boundary effects play a role, with the extreme limit of a linear chain of localized scatterers. By comparing the theoretical results with measurements of the emission angle of the Bragg-reflected light, we show that our optical lattice is very close to the latter case. This case is characterized by the fact that it is hard to detune the light scattering away from the Bragg condition, because the emission angle self-adjusts to the Bragg condition. This can have undesired consequences for the probing of 1D photonic bandgaps predicted to appear in optical lattices as a consequence of multiple reflections between subsequent layers [13,14]. Indeed, their signatures are most conveniently probed at a detuned Bragg angle, such that the band edge spectrally lies outside the resonance frequency of the atomic transition. In this way, the region close to the atomic transition, where multiple reflection competes with diffuse light scattering [3] can be avoided. This is not possible, if the lattice is close to being a chain of point scatterers. Ways to overcome this problem include the choice of larger beam diameter for the dipole trap (eventually by confining the atoms in higher-order transverse electromagnetic modes [10]), smaller Bragg angles, and longer lattices.

We acknowledge financial support from the Landesstiftung Baden-Württemberg.

- 
- [1] E. O. Wollan, *Rev. Mod. Phys.* **4**, 205 (1932).
  - [2] P. S. Jessen and I. H. Deutsch, *Adv. At., Mol., Opt. Phys.* **37**, 95 (1996).
  - [3] G. Birkel, M. Gatzke, I. H. Deutsch, S. L. Rolston, and W. D. Phillips, *Phys. Rev. Lett.* **75**, 2823 (1995).
  - [4] M. Weidemüller, A. Hemmerich, A. Görlitz, T. Esslinger, and T. W. Hänsch, *Phys. Rev. Lett.* **75**, 4583 (1995).
  - [5] S. Slama, C. von Cube, B. Deh, A. Ludewig, C. Zimmermann, and Ph. W. Courteille, *Phys. Rev. Lett.* **94**, 193901 (2005).
  - [6] M. Ben Dahan, E. Peik, J. Reichel, Y. Castin, and C. Salomon, *Phys. Rev. Lett.* **76**, 4508 (1996).
  - [7] M. Greiner, O. Mandel, T. Esslinger, T. W. Hänsch, and I. Bloch, *Nature (London)* **415**, 39 (2002).
  - [8] B. Paredes *et al.*, *Nature (London)* **429**, 277 (2004).
  - [9] C. Fort *et al.*, *Phys. Rev. Lett.* **90**, 140405 (2003).
  - [10] D. Kruse *et al.*, *Phys. Rev. A* **67**, 051802(R) (2003).
  - [11] B. Nagorny *et al.*, *Phys. Rev. A* **67**, 031401(R) (2003).
  - [12] J. M. Coley, *Diffraction Physics* (North-Holland Personal Library, Amsterdam 1995).
  - [13] I. H. Deutsch, R. J. C. Spreeuw, S. L. Rolston, and W. D. Phillips, *Phys. Rev. A* **52**, 1394 (1995).
  - [14] D. V. van Coevorden, R. Sprik, A. Tip, and A. Lagendijk, *Phys. Rev. Lett.* **77**, 2412 (1996).